ADVANCES IN APPLIED MATHEMATICS **10**, 285–323 (1989)

Riemann Problems Requiring a Viscous Profile Entropy Condition

MARIA ELASIR SEABRA GOMES*

Department of Mathematics, Courant Institute of Mathematical Sciences, New York University, New York, 10012

The Riemann problem is solved for 2×2 systems of non-strictly hyperbolic conservation laws abstracted from a three-phase Buckley–Leverett model for oil reservoir flow. The example presented here completes a program for the solution of Riemann problems with quadratic flux functions by allowing the region of parameters most relevant for oil reservoirs. In this example there are shocks which have viscous profiles but do not satisfy the Lax conditions and shocks which satisfy the Lax entropy conditions but fail to have viscous profiles. Therefore these two fundamental notions of entropy are properly distinct. Combining results from numerical and theoretical examinations, we show that the Lax entropy condition is incomplete in this example. The Riemann problem in general fails to have a solution in the class of Lax shocks; the solution of the Riemann problem, however, exists and is in the class of shocks with viscous profiles. Global analysis of dynamical systems defined by traveling wave solutions to the associated viscosity equation is an essential tool for our study. The shapes of the Hugoniot loci were obtained numerically. Numerical methods were also used to distinguish between and show the actual occurrence of all distinct phase configurations which the mathematical theory allowed.

1. INTRODUCTION

In the theory of nonlinear conservation laws, weak solutions are required for an existence theory but they are not uniquely determined by the initial data. Supplementary conditions, known as entropy conditions, are then imposed on the weak solutions to obtain uniqueness. The Lax entropy conditions [10] restrict the characteristics which enter and leave a discontinuity (shock wave). The viscosity admissibility condition restricts allowed discontinuities to be limits of traveling waves for an associated parabolic

*Permanent address: Departamento de Matemática, Universidade Federal de Minas Gerais, Belo Horizonte, 30161 MG, Brazil. Supported by the Conselho Nacional de Pesquisas, Brazil.

0196-8858/89 $7.50

equation, or in the language of this subject, to admit an internal structure [3]. The Lax conditions fail to allow existence while, for the Riemann problem considered here, the viscous profiles give existence of solutions for the Riemann problem.

The example we consider describes the flow of three immiscible incompressible fluids in a porous medium. This model was abstracted from a three-phase Buckley–Leverett model for oil reservoir flow. The flux functions are represented by a quotient of polynomials of degree two. The model has a unique umbilic point, *i.e.*, a state value for which the characteristic speeds coincide. The example we study in the local behavior of these flux functions near the umbilic point, which is described by homogeneous quadratic flux functions [14]. It completes a program for the solution of the Riemann problem for quadratic flux functions by allowing the parametric region most relevant for oil reservoirs. The results presented here are based on our thesis [6]. We thank M. Shearer for pointing out an error in [6] and in a preliminary draft of this paper. The chronological relation between our results and Shearer's is as follows. Our solution of the Riemann problem (with an error in the analysis of saddle–saddle bifurcations) were given in 1987. Shearer's correction to this error and a full solution of the Riemann problem appeared in a 1988 preprint. The present paper was revised on this basis. The intellectual relation is that Shearer depends on our analysis of the vector field at infinity; we require his analysis of saddle–saddle bifurcations. Other aspects of the solution were obtained independently and follow the lines of our original 1987 thesis.

The model studied is introduced in Section 1.1, where some general facts and preliminary results on shock waves are described. The definition of viscous profiles is introduced in Section 2.1. We consider the shocks which are limits of traveling wave solutions of an associated parabolic viscosity equation. These shocks correspond to certain phase space configurations of an associated vector field which depends on two given states U_L and U_R. Section 2.2 is devoted to describing the singularities of the vector field, including those at infinity. There are six singularities of the vector field at infinity, whereas there are at most four singularities on the finite part of the plane. If the vector field has four singularities, three are saddles and the other is a repeller or an attractor. In Section 2.3 we exhibit saddle–saddle connections and determine all such connections. They represent shocks which have viscous profiles but which are not Lax shocks. In Section 2.4, we describe all existing configurations for the dynamical system and use global analysis to draw the phase space of this vector field for any given U_L and U_R. In Section 3 we describe the rarefaction and shock curves. We determine certain loci separating regions where the shock curves have different behavior. The construction of the solution of the Riemann problem is presented in Section 4, based on numerical as well as analytic reasoning. In the solutions we employ profilable shocks which are not Lax shocks. Also, we exhibit Lax shocks which do not satisfy the viscosity admissibility condition. In Appendix A we prove that all saddle–saddle connections which are straight lines lie on the bifurcation lines. If the vector field has four singularities, we show that there are two possibilities:

(i) The three saddles are connected to the singularity which is not a saddle (repeller or attractor).

(ii) Only two saddles are connected to the singularity which is not a saddle (repeller or attractor).

For the computational part of this paper we used the code "Package for the Solution of Riemann Problems," developed by Isaacson, Marchesin, Plohr and Temple [9]. This package determines computationally the solution of the Riemann problem through the construction of wave curves and bifurcation boundaries of the wave curves.

1.1. *Weak Solutions*

Consider a system of two conservation laws in one spatial dimension:

$$U_t + Q(U)_x = 0, \qquad -\infty < x < \infty, \quad t > 0. \tag{1.1}$$

Here $U = U(x,t) = (u,v) \in R^2$ and $Q = (F,G)\colon R^2 \to R^2$ is smooth. The Riemann problem is the initial value problem for this equation with the data

$$U(x,0) = \begin{cases} U_L, & \text{if } x < 0, \\ U_R, & \text{if } x > 0. \end{cases}$$

By a solution of the Riemann problem we mean a function $U = U(x/t)$ consisting of constant states separated by shock, rarefaction and composite waves which we will describe in Section 3.

The system (1.1) is called hyperbolic if the Jacobian matrix dQ of Q has real eigenvalues for $U = (u,v)$. Points where the eigenvalues are equal are called umbilic points.

In this paper we solve the Riemann problem for Q a homogeneous polynomial of second degree subject to the restrictions given below:

$$Q = (F,G) = dC, \qquad \text{where } C = \tfrac{1}{3}au^3 + bu^2v + uv^2 \text{ with } 4a < 3b^2. \tag{1.2}$$

The model (1.2) satisfies

$$\det(dQ(U)) < 0 \qquad \forall U \neq 0. \tag{1.3}$$

In fact, substituting the values of the partial derivatives of F and G we have

$$\det(dQ(U)) = 4\left[-v^2 - buv + (a - b^2)u^2\right].$$

Since the discriminant of $\det(dQ(U))$ is $4a - 3b^2$, we obtain that $\det(dQ(U)) < 0$ for all $U \neq 0$ if $4a - 3b^2 < 0$.

By (1.3), the point $U = 0$ is the unique point where the eigenvalues coincide, *i.e.*, the unique umbilic point. Moreover (a, b) is in region I of the classification in [14].

A function $U = U(x, t)$ is called a weak solution of the system (1.1) if U and $Q(U)$ are integrable functions in each bounded subset of the half-plane $t \geq 0$ and the relationship

$$\int_0^{\infty} \int_{-\infty}^{\infty} [\Phi_t U + \Phi_x Q(U)]\, dx\, dt + \int_{-\infty}^{\infty} \Phi(x,0) U(x,0)\, dx = 0$$

holds for every smooth test function Φ with compact support in $t \geq 0$ [10].

Using the divergence theorem one can prove the following lemma: let $[U] = U^{+} - U^{-}$ denote the jump across a curve of discontinuity and let s be the speed of propagation of the discontinuity. If U is a piecewise smooth weak solution of (1.1) then across the discontinuity the jump relationship $s[U] = [Q]$, which is also called Rankine–Hugoniot relation R–H, holds.

In particular, a piecewise constant weak solution to (1.1), called shock solution, with a single jump across the line $x = st$,

$$U(x, t) = \begin{cases} U_L, & \text{if } x < st; \\ U_R, & \text{if } x > st; \end{cases}$$

must satisfies R–H relation:

$$\mathscr{H}_{U_L}(s, U_R) \equiv -s(U_R - U_L) + Q(U_R) - Q(U_L) = 0.$$

Fix U_L in the R–H relation above. For all s, $U_R = U_L$ satisfies the R–H relation; it corresponds to a constant solution $U(x, t) = U_L$. The characterization of the locus $\{(s, U): \mathscr{H}_{U_L}(s, U) = 0\}$ in a neighborhood of U_L is obtained as follows.

At the point $s = \lambda_k(U_L)$, $U = U_L$, the matrix $d\mathscr{H}_{U_L}$ is singular; so this is a bifurcation point for this locus. Here the eigenvalues and right eigenvectors of $dQ(U)$ are denoted λ_k, r_k, $k = 1$ or 2, respectively. Let us consider first the case when U_L is not an umbilic point, that is, $\lambda_k(U_L)$ is a simple eigenvalue. By the Crandall–Rabinowitz theorem [4], there exists a smooth primary branch $\{(s(\varepsilon), U(\varepsilon)), |\varepsilon| < \delta\}$ of this locus such that:

(a) $\mathscr{H}_{U_L}(s(\varepsilon), U(\varepsilon)) = 0$.

(b) $s(0) = \lambda_k(U_L)$, $U(\varepsilon) = U_L$ if and only if $\varepsilon = 0$.

(c) $\dot{s}(0) = \frac{1}{2}\dot{\lambda}_k(0)$, $\dot{U}(0) = r_k(U_L)$.

(d) There is a neighborhood η of $(\lambda_k(U_L), U_L)$ such that if $(s, U) \in \eta$ and $\mathscr{H}_{U_L}(s, U) = 0$ and then either $U = U_L$ or $(s, U) = (s(\varepsilon), U(\varepsilon))$ for some ε, with $|\varepsilon| < \delta$.

Let us consider now the case when U_L is the umbilic point, so that $\lambda_1(U_L) = \lambda_2(U_L)$ is a double eigenvalue. If moreover, $dQ(U_L)$ is diagonalizable then $\mathscr{H}_{U_L}(s, U) = 0$, near $(s = \lambda_k(U_L), U = U_L)$, consists generically of one or three primary branches [11].

Eliminating the value of s in the R–H relation we obtain

$$[F(U) - F(U_L)](v - v_L) - [G(U) - G(U_L)](u - u_L) = 0. \quad (1.4)$$

This locus, which is the projection of $\mathscr{H}_{U_L}(s, U) = 0$ onto the U_R-plane, is called the Hugoniot locus. For flux functions which are homogeneous polynomials, the Hugoniot locus through the umbilic point $U_L = (0,0)$ is the union of straight lines satisfying

$$s = \frac{F(U)}{u} = \frac{G(U)}{v}, \qquad \text{where } U = (u, v). \quad (1.5)$$

The slopes of these lines are roots of the equations:

$$\alpha F(1, \alpha) - G(1, \alpha) = 0 \qquad \text{or} \qquad F(\alpha, 1) - \alpha G(\alpha, 1) = 0. \quad (1.6)$$

For the models introduced above it is easy to check that Eqs. (1.6) have three distinct real roots. We denote these lines the bifurcation lines. The reason for this terminology is that in the model (1.2) the Hugoniot locus through U_L has a point of secondary bifurcation if and only if U_L lies on one of these lines [15].

2. Viscous Profiles

2.1. *Introduction*

One approach to obtain the elementary shock waves which arise in the solutions of the Riemann problem for a hyperbolic system of conservation laws is to derive these elementary solutions as limits of traveling wave solutions of an associated parabolic equation. In this paper we consider the approximating parabolic equation

$$U_t + Q(U)_x = \varepsilon U_{xx}, \qquad \varepsilon > 0, \tag{2.1}$$

called the viscosity equation associated with (1.1). Gel'fand [5] showed that the existence of such shocks corresponds to certain configurations of the phase space of an ordinary differential equation. More specifically, let U_L and U_R be two constant states that can be connected through a shock with speed s. We seek smooth solutions of (2.1) of the form $U = U((x - st)/\varepsilon)$ which converge as ε tends to zero to the given weak solution of (1.1). Substituting

$$U = U(\xi), \qquad \xi = \frac{x - st}{\varepsilon}$$

in the viscosity equation (2.1), we see that U satisfies the second-order ordinary differential equation

$$-sU_\xi + Q(U)_\xi = U_{\xi\xi}.$$

This equation can be integrated once to yield

$$-sU + Q(U) + C = \dot{U}. \tag{2.2}$$

Here C is a constant and the superimposed dot indicates differentiation with respect to ξ. If $U = U(\xi)$ converges to the shock solution of $U_t + Q(U)_x = 0$ when $\varepsilon \to 0$, we must have

$$\lim_{\xi \to -\infty} U(\xi) = U_L \qquad \text{and} \qquad \lim_{\xi \to +\infty} U(\xi) = U_R.$$

It follows that the left-hand side of (2.2) must vanish at U_L and U_R. Therefore, we can find the value of $C = sU_L - Q(U_L)$ and (2.2) becomes

$$\dot{U} = -s(U - U_L) + Q(U) - Q(U_L). \tag{2.3}$$

The system (2.3) may be written as

$$\begin{aligned} \dot{u} &= -s(u - u_L) + F(U) - F(U_L) \equiv \Phi(U), \\ \dot{v} &= -s(v - v_L) + G(U) - G(U_L) \equiv \Psi(U). \end{aligned} \tag{2.4}$$

From now on X_s will denote the vector field (Φ, Ψ), with Φ and Ψ as above. Notice that U_L and U_R are singularities of this vector field and that all singularities of X_s lie on the Hugoniot locus. The singularities of X_s depend on s (as well as on U_L and U_R). We recall the following definition.

DEFINITION 2.1. Let γ be the orbit through a point p of a C' vector field X on the plane. The ω-limit of p is the set

$$\omega(p) = \{q \in R^2; \exists \tau_n \to \infty \text{ with } \gamma(\tau_n) \to q\}.$$

We note that $\omega(p) = \omega(\tilde{p})$ if $\tilde{p}$ belongs to the orbit of p. We define the ω-limit of an orbit as the set of $\omega(p)$ for any $p \in \gamma$. Similarly, we define the α-limit for $\tau_n \to -\infty$.

Therefore, for the existence of a shock wave solution of $U_t + Q(U)_x = 0$ which is a limit of traveling wave solutions of the associated parabolic equation (2.1) there must exist an orbit γ of the vector field $X_s = (\Phi, \Psi)$ satisfying

$$\alpha(\gamma) = U_L \qquad \text{and} \qquad \omega(\gamma) = U_R.$$

We say that a shock s, U_L, U_R has a viscous profile if there exists an orbit of the vector field $X_s = (\Phi, \Psi)$ connecting U_L to U_R.

We say that a singularity p of a vector field X is hyperbolic if the eigenvalues Λ_1 and Λ_2 of the linear vector field $dX(p)$ have non-zero real part. When the eigenvalues of $dX(p)$ are real, a hyperbolic singularity is an attractor if $\Lambda_1 \leq \Lambda_2 < 0$, a repeller if $0 < \Lambda_1 \leq \Lambda_2$ and a saddle if $\Lambda_1 < 0 < \Lambda_2$. We remark that the eigenvalues of dX_s are $-s + \lambda_k(U)$, $k = 1, 2$. Thus the singularities of X_s fail to be hyperbolic when $s = \lambda_k(U)$, $k = 1, 2$. For a Lax 1-shock (or slow shock) [10],

$$s < \lambda_1(U_L) \qquad \text{and} \qquad \lambda_1(U_R) < s < \lambda_2(U_R),$$

or equivalently U_L is a repeller and U_R is a saddle. For a Lax 2-shock (or fast shock)

$$\lambda_1(U_L) < s < \lambda_2(U_L) \qquad \text{and} \qquad \lambda_2(U_R) < s,$$

or in other words U_L is a saddle and U_R is an attractor. For overcompressive shocks, defined by

$$\lambda_2(U_R) < s < \lambda_1(U_L),$$

U_L is a repeller and U_R is an attractor. For crossing shocks defined by

$$\lambda_1(U_L) < s < \lambda_2(U_L) \qquad \text{and} \qquad \lambda_1(U_R) < s < \lambda_2(U_R),$$

the two singularities are saddles. Lax shocks can be regarded as shocks which are clearly associated with a single characteristic family. For a Lax shock, this characteristic family is the same when viewed from either side of the shock. Neither the overcompressive nor the crossing shocks are Lax shocks.

We will prove that for the model (1.2) there exist crossing shocks which have viscous profiles (Theorem 2.6), as well as Lax shocks which do not have viscous profiles (Theorem 4.4). Thus we conclude that Lax shocks and shocks with viscous profiles are properly distinct concepts. Furthermore all possible saddle–saddle connections are completely characterized as segments of bifurcation lines. To determine all shocks that have viscous profiles we will draw the phase space of the vector field X_s for all U_L and U_R. To this end we will study the singularities of the vector field, the asymptotic behavior of unlimited orbits, and the existence of saddle–saddle connections.

All the results of Sections 2.2–2.4 are established as mathematical theorems.

2.2. *Singularities of the Vector Field X_s*

In this section, we determine the number and type of the singularities, including those at infinity, for the vector field associated with (1.2). There are six singular points of X_s at infinity, independent of s (Theorem 2.2). In the finite part of the (u, v)-plane, generically there are two or four singularities, while three singularities arise as a degenerate case. All singularities are classified as to type (saddle, attractor, etc.). This analysis of X_s is the technical foundation for our main results.

To study the asymptotic behavior of the unlimited orbits of a vector field X on the plane, we use the Poincaré transformation described below [1]. Consider

$$S^2 = \{(x_1, x_2, x_3) \in R^3;\ x_1^2 + x_2^2 + x_3^2 = 1\}$$

and

$$\pi = \{(x_1, x_2, x_3) \in R^3;\ x_3 = -1\};$$

i.e., π is the tangent plane to the unit sphere S^2 at the south pole $(0, 0, -1)$. Any straight line joining the origin $(0, 0, 0)$ and a point on the plane π intercepts S^2 at two antipodal points. Reciprocally, any antipodal points not on the equator $x_3 = 0$ define exactly one point on the plane π. If X is a vector field on the plane π, the mapping above induces a vector field on the sphere minus the equator.

Let $\pi_1 = \{(x_1, x_2, x_3) \in R^3;\ x_1 = 1\}$. We introduce coordinates w and z on this plane, with origin at $(1, 0, 0)$; the w-axis and z-axis parallel to the x_2-axis and the x_3-axis, respectively. The w-axis has the same direction as the x_2-axis and the z-axis has the opposite direction to the x_3-axis, as shown in Fig. 2.1.

By the transformation above, to any two antipodal points, out of the plane $x_1 = 0$ parallel to π_1, there corresponds a point on the plane π_1. If

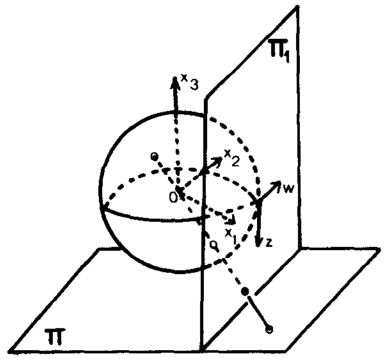

FIGURE 2.1

$(x_1, x_2, -1)$ is a point on the plane π the corresponding point on π_1 by the transformation above is given by

$$w = x_2/x_1, \qquad z = 1/x_1 \qquad \text{if } x_1 \neq 0. \tag{2.5}$$

For $x_1 = 0$ we consider instead of π_1 the plane $\pi_2 = \{(x_1, x_2, x_3) \in R^3\colon x_2 = 1\}$. Similarly, a point $(x_1, x_2, -1)$ on the plane π corresponds to a point on π_2 given by

$$w = x_1/x_2, \qquad z = 1/x_2 \qquad \text{if } x_2 \neq 0. \tag{2.6}$$

Note that the points at infinity correspond to $z = 0$.

THEOREM 2.2. *Let Q be the quadratic polynomial* (1.2). *Then the vector $X_s = (\Phi, \Psi)$ has six singularities at infinity; three are attractors and three are repellers.*

Proof. Let $u \neq 0$. Applying the Poincaré transformation (2.5) $u = 1/z$ and $v = w/z$ to the vector field X_s, we obtain

$$\begin{aligned}\frac{dw}{d\tau} &= -wz\Phi(1/z, w/z) + z\Psi(1/z, w/z)\\ &= \frac{1}{z}\{-w[-sz(1 - zu_L) + F(1, w) - z^2F(U_L)]\\ &\qquad + G(1, w) - z^2G(U_L) - sz(w - zv_L)\}, \qquad (2.7)\\ \frac{dz}{d\tau} &= -z^2\Phi(1/z, w/z)\\ &= -\{-sz(1 - zu_L) + F(1, w) - z^2F(U_L)\}.\end{aligned}$$

Multiplying the left-hand side of the two equations above by z and making the substitution $\tau = z\zeta$, we get

$$\begin{aligned}\frac{dw}{d\zeta} &= -w\left[-sz(1 - zu_L) + F(1, w) - z^2F(U_L)\right]\\ &\quad + G(1, w) - z^2G(U_L) - sz(\omega - zv_L), \qquad (2.8)\\ \frac{dz}{d\zeta} &= -z\left[-sz(1 - zu_L) + F(1, w) - z^2F(U_L)\right].\end{aligned}$$

Note that this vector field can be extended analytically to the equator. The points on the equator represent the points at infinity of the plane. So the singularities at infinity ($w, z = 0$), if existent, satisfy $-wF(1, w) + G(1, w) = 0$. By (1.6), the last equation has three roots $w = \alpha_i$, $i = 1, 2, 3$ for the model (1.2). The Jacobian matrix of the vector field (2.8) evaluated at these singularities is

$$\begin{pmatrix} \Upsilon'(\alpha_i) & \Theta(\alpha_i) \\ 0 & \Gamma(\alpha_i) \end{pmatrix},$$

where

$$\begin{aligned}\Upsilon'(w) &= -F(1, w) - wF'(1, w) + G'(1, w),\\ \Gamma(w) &= -F(1, w).\end{aligned}$$

Hence, the eigenvalues at the singularities are real. To show that they are either attractors or repellers we will show that $\Upsilon'(\alpha_i)\Gamma(\alpha_i) > 0$, $i = 1, 2, 3$.

Let $H(w) \equiv -wF(1, w) + G(1, w)$. Thus, $H'(w) = \Upsilon'(w)$. By (1.2) the zeros of $F(1, w)$ are interspersed with the zeros (α_1, α_2, and α_3) of $H(w)$, as shown in Fig. 2.2. Hence, $\Upsilon'(\alpha_i)\Gamma(\alpha_i) = -H'(\alpha_i)F(\alpha_i) > 0$, $\Upsilon'(\alpha_2) > 0$, and $\Upsilon'(\alpha_i) < 0$, $i = 1$ or 3. Consequently, α_2 is a repeller; α_1 and α_3 are attractors.

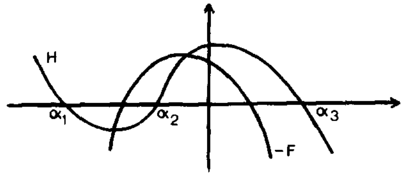

FIGURE 2.2

If $u = 0$, using the other Poincaré transformation (2.6) we have that the points $(1,0)$ and $(-1,0)$ are not singularities of the vector field on the sphere.

Each point $(\alpha_i, 0)$, $i = 1,2,3$, corresponds to two antipodal points of the sphere. Since the vector field (2.7) was multiplied by z, the directions of the vector field at antipodal points are reversed [1]. Therefore there are three repellers and three attractors. □

We now determine the number and type of the singularities of the vector field X_s for the model (1.2) on the finite part of the plane.

The singularities of $X_s = (\Phi, \Psi)$ are the points (u, v) for which

$$\Phi(u,v) = F(u,v) - su - F(u_L, v_L) + su_L = 0,$$
$$\Psi(u,v) = G(u,v) - sv - G(u_L, v_L) + sv_L = 0.$$

Substituting the values of F and G (1.2), we can see that $\Phi = 0$ and $\Psi = 0$ are hyperbolas, since $4a < 3b^2$. Therefore the singularities of the vector field X_s are the intersection of these hyperbolas.

We observe that if these hyperbolas happen to be tangent, the tangency points satisfy $s = \lambda_k(U)$, $k = 1,2$. In fact, if U is a tangency point then $\nabla\Phi$ is parallel to $\nabla\Psi$ at this point or equivalently

$$\det\begin{vmatrix} F_u - s & F_v \\ G_u & G_v - s \end{vmatrix} = 0.$$

Thus, we obtain that $s = \lambda_k(U)$, $k = 1$ or 2. Note that the singularities of the vector field fail to be hyperbolic at the tangency points.

The next theorem gives the types of the singularities of X_s, on the finite part of the plane.

THEOREM 2.3. *The vector field X_s has two, three, or four singularities in the finite part of the plane.*

(i) *If the vector field X_s has four singularities then three singularities are saddles and the other is an attractor or a repeller.*

(ii) *If the vector field X_s has three singularities then two singularities are saddles and the other singularity is a saddle-node* [1].

(iii) *If the vector field X_s has two singularities then both are saddles.*

Proof. The construction of the vector field X_s ensures that it has at least two singularities (U_L and U_R). Since the singularities are the intersection points of the hyperbolas the vector field has at most four singularities.

First, we suppose that X_s has four singularities. In other words, the hyperbolas are transversal in which case all singularities are hyperbolic.

By the Poincaré transformation (2.5)–(2.6) we can consider the vector field X_s on the sphere. Using the Poincaré–Hopf theorem the sum of the indices of the singularities of the vector field X_s is $+2$, the Euler characteristic of the sphere [12]. Each singularity of X_s on the plane corresponds to two antipodal singularities on the sphere. Thus X_s has eight singularities coming from the finite part of the plane and six singularities coming from infinity. The singularities at infinity are attractors or repellers (Theorem 2.2). But the index is $+1$ in the case of a node (repeller or attractor) and -1 in the case of a saddle. Therefore $2 = 6 + 2x - 2y$, where x is the number of nodes, and y is the number of saddles on the finite part of the plane. Since $x + y = 4$ we obtain $x = 1$ and $y = 3$. Hence there are three saddles and one node on the finite part of the plane.

Similarly if the vector field has two singularities then both singularities are saddles.

In the degenerate case of the vector field with three singularities then the hyperbolas are tangent, and one can show that two singularities are saddles and the non-hyperbolic signularity is a saddle-node (index zero). □

2.3. *Saddle–Saddle Connections*

Our main tool in this study is Theorem 2.6, which completely identifies all possible saddle–saddle connections. We exhibit crossing shocks which have viscous profiles. In other words, we show that there exist orbits connecting two saddles. Furthermore, all possible saddle–saddle connections are completely characterized as segments of the bifurcations lines. In Appendix A we prove the lemma below.

LEMMA 2.4. *Let $Q = (F, G)$, where $F(U)$ and $G(U)$ are homogeneous polynomials of degree $2n$, with no common factor, such that* $\det(dQ(U)) < 0$ *for $U \neq 0$. Let X_s be the vector field associated with Q. Then*:

(a) *There exist U_L and s such that the vector field X_s has saddles which are connected by an orbit.*

(b) *All saddles of the vector field X_s lying on a common bifurcation line are connected by an orbit.*

(c) *All saddle–saddle connections of X_s which are straight lines lie on a common bifurcation line.*

Chicone in [2] proved Theorem 2.5 below, for quadratic gradient vector fields $X = (\Phi, \Psi)$ on the plane, where Φ and Ψ are relatively prime polynomials. All quadratic vector fields on the plane which have connections between two saddle points and with more than one pair of singularities at inifinity are classified in [7]. Moreover, it is shown that, in general there are orbits connecting two saddles which are straight line segments.

THEOREM 2.5. *Let $X = (\Phi, \Psi)$ be a quadratic vector field on the plane, where Φ and Ψ are relatively prime polynomials. Every orbit connecting two saddles of X is a straight line segment.*

Combining Lemma 2.4 and Theorem 2.5 we obtain the theorem below.

THEOREM 2.6. *For the model* (1.2) *the vector field X_s has saddle–saddle connections and the connections necessarily lie on a common bifurcation line. Moreover, all saddles lying on a common bifurcation line are connected by an orbit.*

Proof. By (1.3) $\det(dQ(U)) < 0$ for all $U \neq 0$. It is easy to see that the flux function components do not have common factors. From Lemma 2.4 we obtain that there are saddle–saddle connections and all saddles lying on the common bifurcation line are connected by an orbit. Using Theorem 2.5 every orbit connecting saddles of X_s is a straight line segment. Again by Lemma 2.4, we obtain that this straight line segment lies on a common bifurcation line. □

2.4. *Phase Space Configurations*

Given states U_L and U_R, the vector field X_s is characterized by the properties of Sections 2.2 and 2.3. This knowledge allows us to understand the phase space configuration of X_s.

The main point of this section is to determine which shocks are profilable. We showed that crossing shocks (shocks for which U_L and U_R are both saddles) have viscous profiles if and only if they lie on a common bifurcation line (Theorem 2.6). We have already proven that in the case of shocks for which one of U_L or U_R is either a repeller or an attractor the vector field X_s has four singularities, three being saddles (Theorem 2.3). In Appendix A we prove that in this case there are two possibilities which are described in the two theorems below. In the model (1.2), for all s, the vector field X_s does not have both an attractor and a repeller. Hence there exist no overcompressive shocks.

THEOREM 2.7. *Assume that the vector field X_s has four singularities and that there are no saddle–saddle connections. Then at least two saddles are connected to the repeller* (*or attractor*).

THEOREM 2.8. *Assume that X_s has four singularities and that there are saddle–saddle connections. Then only two saddles are connected to the repeller* (*or attractor*).

3. The Nonlinear Wave Curves

In this section we describe the wave curves for the model (1.2). The rarefaction and shock curves are drawn. We determine certain boundaries where these curves change behavior. The major new result is the analytical proof of the existence of the hysteresis locus. The shape of the Hugoniot loci, which are also new for the present case, are obtained numerically. It is shown in [14] that the qualitative behavior of the rarefaction curves is as given in Fig. 3.1.

3.1. *Rarefaction Wave Curves*

Rarefaction curves in state space correspond to smooth solutions of the form $U = U(x/t)$ which satisfy (1.1) in physical space. The value $U(\xi)$ must lie on an integral curve of some eigenvector field $r_k(U)$, $k = 1, 2$ while $\xi = x/t$ is the characteristic speed $\lambda_k(U(\xi))$. Thus $\lambda_k(U(\xi))$ has to grow monotonically with ξ as the state U moves from left to right in physical space. The oriented integral curves are called rarefaction curves. Such curves are shown in Fig. 3.1.

A critical point U of λ_k, $k = 1$ or 2, on the rarefaction curve is called a point of inflection. Such point U satisfies $\nabla\lambda_k(U) \cdot r_k(U) = 0$. The set of inflection points is called the *inflection locus*.

Since system (1.2) is homogeneous, the inflection loci are straight lines through the origin. As shown in [15], in region I the inflection locus for each family ($k = 1$ or 2), consists of three half lines I_i^k, $i = 1, 2, 3$, where I_i^1 is the half line opposite to I_i^2.

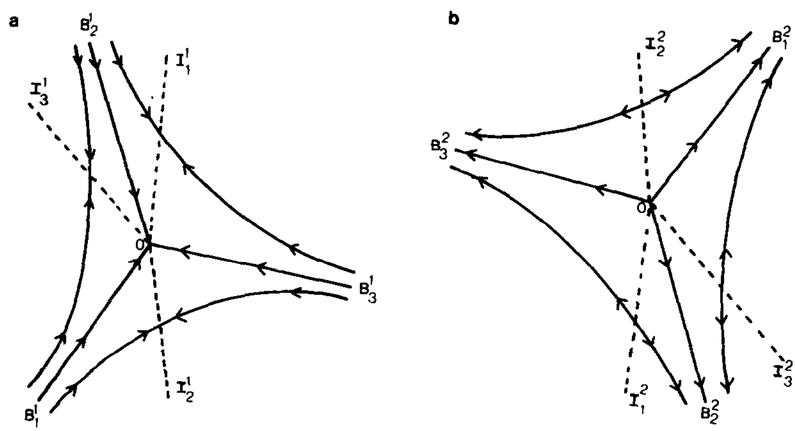

FIG. 3.1. (a) Slow rarefaction; (b) Fast rarefaction.

We denote $R_k(U_L)$ the part of the k-rarefaction curve through U_L such that, starting from U_L, λ_k increases monotonically.

3.2. *Shock Wave Curves*

Let U_L be fixed. The set of points on the Hugoniot locus through U_L which are connected to U_L by an orbit is called the shock curve. Note that this curve depends on U_L.

The admissibility of a shock is related to the signs of $\lambda_k(U_L) - s(U_L, U)$ and $\lambda_k(U) - s(U_L, U)$, $k = 1, 2$. This leads us to analyze the transition points where $\lambda_k(U_L) = s$ or $\lambda_k(U) = s$. As we have seen in Section 1, $s = \lambda_k(U_L)$, $k = 1, 2$ are bifurcation points on the trivial solution $U = U_L$, s variable. The following theorem shows the relation between $s = \lambda_k(U)$ and $\dot{s}$, the derivative of s along $\mathscr{H}_{U_L} = 0$ [20].

THEOREM 3.1. *Let $l_k(U)$ denote a left eigenvector of $dQ(U)$ corresponding to the eigenvalue $\lambda_k(U)$ $(k = 1, 2)$. Suppose that $\langle l_k(U), U - U_L\rangle \neq 0$ and $\mathscr{H}_{U_L}(s, U) = 0$. Then $s = \lambda_k(U)$ if and only if $\dot{s} = 0$.*

Proof. Differentiating along $\mathscr{H}_{U_L} = 0$ gives $(dQ(U) - sI)\dot{U} = \dot{s}(U - U_L)$. Multiplying this equation by $l_k(U)$ gives

$$(\lambda_k(U) - s)\langle l_k(U), \dot{U}\rangle = \dot{s}\langle l_k(U), U - U_L\rangle.$$

Since $\langle l_k(U), U - U_L\rangle \neq 0$ then $\dot{s} = 0$ if and only if $s = \lambda_k(U)$. □

When $\langle l_k(U), U - U_L\rangle = 0$ and $s = \lambda_k(U)$, $k = 1, 2$ we have $\operatorname{rank}(d\mathscr{H}_{U_L}) < 2$. In this case U is called a secondary bifurcation point, since it happens on a non-trivial branch. In [15], it was shown that there exists a secondary bifurcation point if and only if U_L lies on the Hugoniot locus through the umbilic point. There are three secondary bifurcation lines B_i^k, $i = 1, 2, 3$ and $k = 1, 2$ where B_i^1 and B_i^2 are opposite half lines.

As was seen in [15], on the U_L-plane the Hugoniot locus changes qualitatively across the inflection and bifurcation lines. Now we describe two other loci on the U_L-plane across which the Hugoniot locus also changes its behavior. Since the models studied in this paper are homogeneous polynomials we can see that these loci, if they are not empty, are lines.

The double contact locus is

$$D = \{U_L : \exists (s, U), U \neq U_L, \mathscr{H}_{U_L}(s, U) = 0,\\ s = \lambda_k(U_L) = \lambda_j(U), k, j = 1, 2\}.$$

In [15], it was established that the double contact locus is empty.

The hysteresis locus is

$$H = \{U_L : \exists(s, U), U \neq U_L, \mathscr{H}_{U_L}(s, U) = 0, \\ s = \lambda_k(U), \nabla\lambda_k(U) \cdot r_k(U) = 0, k = 1, 2\}.$$

PROPOSITION 3.2. *For $4a < 3b^2$ the hysteresis locus consists of three lines. Opposite halves of these lines are associated with opposite families.*

Proof. Since F and G are homogeneous polynomials, the hysteresis locus is the union of lines through the origin. Opposite halves of the lines are associated with different families. Let $U_L \in I_i^k$. Then $\nabla\lambda_k(U_L) \cdot r_k(U_L) = 0$. A point U is a hysteresis point if $\mathscr{H}_{U_L}(s, U) = 0$ and $s = \lambda_k(U_L)$. That is,

$$s = \frac{F(U) - F(U_L)}{u - u_L} = \frac{G(U) - G(U_L)}{v - v_L} = \lambda_k(U_L).$$

Then we obtain the system

$$\begin{aligned} F(U) - F(U_L) &= \lambda_k(U_L)(u - u_L), \\ G(U) - G(U_L) &= \lambda_k(U_L)(v - v_L). \end{aligned} \tag{3.1}$$

But F and G are polynomials of degree two, so the system above has at most four real roots. We show that U_L is a triple root. Therefore, there is a unique solution $U \neq U_L$ of the system, yielding one hysteresis line for each inflection line.

In fact, substituting the value of $G(u, v) = bu^2 + 2uv$ in the second equation of (3.1) we obtain

$$v \equiv p(u) = \frac{G(U_L) - \lambda_k(U_L)v_L - bu^2}{2u - \lambda_k(U_L)} \qquad \text{if } u \neq \tfrac{1}{2}\lambda_k(U_L).$$

Substituting v in the first equation of (3.1) we define

$$q(u) \equiv F(u, p(u)) - F(U_L) - \lambda_k(U_L)(u - u_L).$$

The point U_L is a triple root of q. In fact, $q(u_L) = 0$ and $q'(u_L) = F_u(U_L) + F_v(U_L)p'(u_L) - \lambda_k(U_L) = 0$, since $p'(u_L)$ is the slope of the eigenvector $r_k(U_L)$. Computing the second derivative we get $q''(u_L) = F_{uu}(U_L) + 2F_{uu}(U_L)p'(u_L) + F_{vv}(U_L)p'^2(u_L) + F_v(U_L)p''(u_L)$. Since $\nabla\lambda_k(U_L) \cdot r_k(U_L) = 0$ and $p'(u_L)$ is the slope of the eigenvector $r_k(U_L)$, we have $F_v(U_L)p''(u_L) = -F_{uu}(U_L) - 2F_{uv}(U_L)p'(u_L) - F_{vv}(U_L)p'^2(u_L)$. Hence

$q''(u_L) = 0$. The third derivative is

$$q'''(u_L) = 3\left[F_{uv}(U_L) + F_{vv}(U_L)p'(u_L)\right]p''(u_L) + F_v(U_L)p'''(u_L).$$

Again, using that $\nabla\lambda_k(U_L) \cdot r_k(U_L) = 0$ and that $p'(u_L)$ is the slope of the eigenvector $r_k(U_L)$ we can show $q'''(u_L) \neq 0$. The proof is complete. □

We denote H_i^j the i-hysteresis line with respect to the j-family.

Since the double contact locus is empty, the U_L-plane is divided by the bifurcation, inflection, and hysteresis loci into eighteen sectors. To illustrate the solution of the Riemann problem we now choose particular values for the parameters (a, b). For this choice these loci were obtained numerically in the counterclockwise sense:

$$B_1^2,\ H_1^2,\ I_1^1,\ I_2^2,\ H_2^1,\ B_2^1,\ I_3^1,\ H_3^2,\ B_3^2.$$

Because of the symmetry in the model, we draw in Fig. 3.2 only the Hugoniot loci for U_L in some regions of the U_L-plane, as well as U_L on the bifurcation line B_1^2. All Lax and crossing shocks are labeled by 1 for 1-shocks, 2 for 2-shocks, and X for crossing shocks. The points a, b, c, and d are points where $s = \lambda_1(U_L)$, $s = \lambda_2(U_L)$, $s = \lambda_1(U)$, and $s = \lambda_2(U)$, respectively.

The Hugoniot locus through U_L, for U_L not on the bifurcation lines, can be parameterized by the angle θ of the polar coordinate system centered at U_L [8]. More specifically, $u = u_L + R\cos\theta$ and $v = v_L + R\sin\theta$, where

$$R \equiv R(\theta) = -2\frac{Au_L + Bv_L}{A\cos\theta + B\sin\theta},$$

with

$$A \equiv b\sin^2\theta + (a-1)\sin\theta\cos\theta - b\cos^2\theta$$

and

$$B = \sin^2\theta + b\sin\theta\cos\theta - \cos^2\theta.$$

The shapes of the Hugoniot loci were verified numerically.

3.3. *Composite Wave Curves*

Let U_L be fixed. For each $U_M \in R_k(U_L)$, where $R_k(U_L)$ is the k-rarefaction curve starting from U_L, we consider the points U on the shock curve through U_M for which $s(U_M, U) = \lambda_k(U_M)$. We call the set of these points U the rarefaction–shock composite curve. Viewed in the physical space

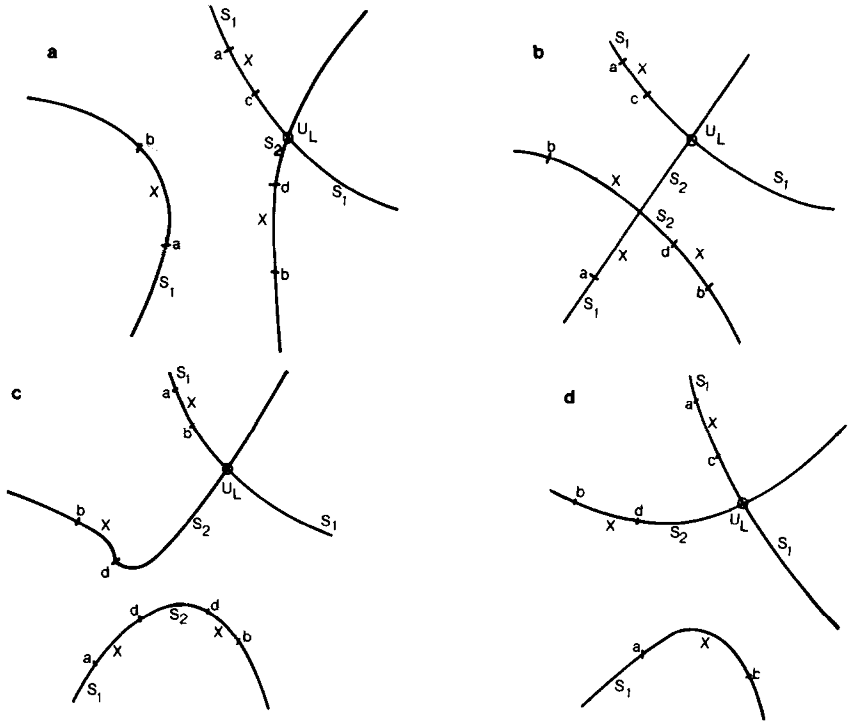

FIG. 3.2. (a) U_L between B_3^1 and B_1^2; (b) U_L on B_1^2; (c) U_L between B_1^2 and H_1^2; (d) U_L between H_1^2 and I_1^1; (e) U_L between I_1^1 and I_2^2; (f) U_L between I_2^2 and H_2^1; (g) U_L between H_2^1 and B_2^1; (h) U_L between B_2^1 and I_3^1.

(x, t) any wave on this curve, which we denote by $(RS)_k$, is a rarefaction fan bordered on the right by a shock. A shock–rarefaction composite curve is the set points $U \in R_k(U_M)$ for U_M on the shock curve through U_L such that $s(U_L, U_M) = \lambda_k(U_M)$. In this case the shock is on the left edge of the rarefaction fan, in the physical space (x, t).

We denote by $W_k(U_L)$ a wave curve representing all states U_R connected to U_L on the right by shock, rarefaction or composite waves of the k-family.

4. Riemann Solution

4.1. *Construction of the Solution*

Let U_L be fixed. To solve the Riemann problem for any U_R we consider all possible successions of waves with U_L on the left. When the sets $W_k(U)$,

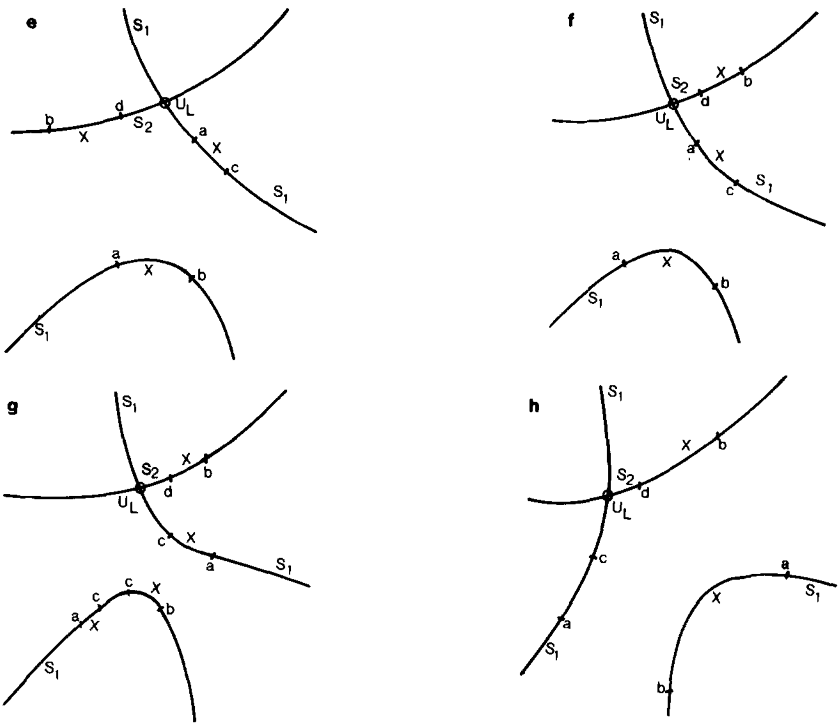

FIG. 3.2—*Continued*

$k = 1, 2$ for all $U \in R^2$ form a coordinate system, we solve the Riemann problem determining a point U_M on $W_1(U_L)$ such that $W_2(U_M)$ contains U_R. In this way the solution of the Riemann problem will be a 1-wave (or slow wave) from U_L to U_M followed by a 2-wave (or fast wave) from U_M to U_R. In this case we would obtain existence and uniqueness as proved by Smoller [19], for strictly hyperbolic and genuinely nonlinear systems. The model showed in this paper does not have this coordinate system.

We show in Fig. 4.1 the regions in the U_R-plane specified according to the wave succession from U_L to U_R for:

(a) U_L between B_3^1 and B_1^2;
(b) U_L between B_1^2 and H_1^2.

We do not show the solution to the Riemann problem in the other regions because they are similar. For each U_L above, we subdivide the U_R-plane in three components, in each of which the construction of the a

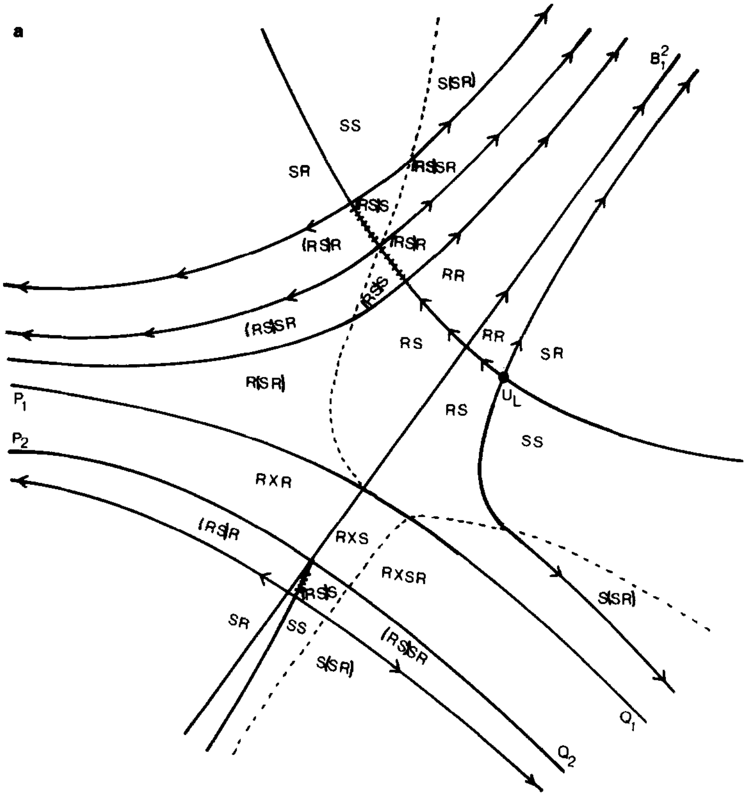

FIGURE 4.1

Riemann problem possesses certain analogies. The fast wave curves $\widehat{P_1Q_1}$ and $\widehat{P_2Q_2}$ are the boundaries of these components. The first component contains U_L, the second contains those crossing shocks which lie on bifurcation lines and the third component contains part of the disconnected branch of $W_1(U_L)$. In Fig. 4.1, the railroad tracks mean a rarefaction–shock composite wave and the dotted lines are the points of transition $s = \lambda_2(U)$. The arrows indicate the increasing direction of the eigenvalues on the rarefaction waves.

We detail the construction of the solution in each component and present some examples. In the first component the solution is obtained as in [18]. The solution corresponds to a slow wave from U_L to U_M, followed by a fast wave from U_M to U_R, where U_M is the point on $W_1(U_L)$ such that $U_R \in W_2(U_M)$. Let us describe in detail the solution for U_L between B_3^1 and H_1^2 and U_R in the region indicated in Fig. 4.2. The solution of the Riemann

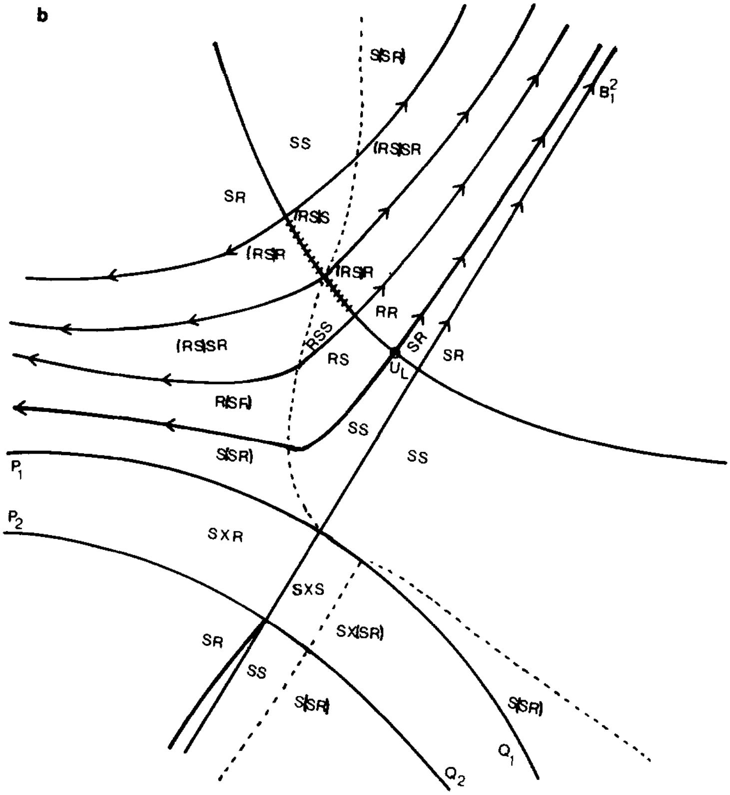

FIGURE 4.1—*Continued*

problem for the given U_L, U_R is represented by the curve consisting of the slow rarefaction–shock composite wave from U_L to U_M, followed by the fast rarefaction wave from U_M to U_R.

For U_R in the second component, the solution is a slow wave from U_L to $U_1{}^* = W_1(U_L) \cap B_k^2$ for some $k = 1, 2, 3$ followed by a crossing shock wave from $U_1{}^*$ to $U_2{}^* \in B_k^1$ such that $U_R \in W_2(U_2{}^*)$ and then a fast wave from $U_2{}^*$ to U_R. For instance, consider U_L between B_1^2 and H_1^2, and U_R in the region indicated in Fig. 4.3. The solution of the Riemann problem for U_L, U_R is represented by the Lax 1-shock wave from U_L to $U_1{}^*$, followed by the crossing shock wave from $U_1{}^*$ to $U_2{}^*$ and then by the Lax 2-shock wave from $U_2{}^*$ to U_R. In this component the solution of the Riemann problem has profilable shocks which do not satisfy Lax conditions.

When U_R belongs to the third component the solution is a slow wave from U_R to U_M, where U_M belongs to the disconnected component of $W_1(U_L)$ and $U_R \in W_2(U_M)$, followed by a fast wave from U_M to U_R as was

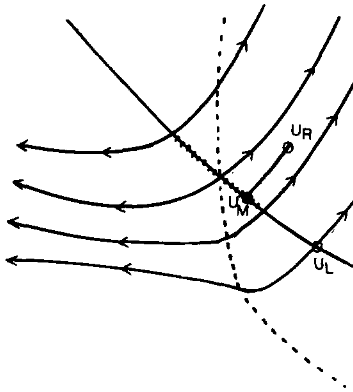

FIGURE 4.2

obtained in [16]. For instance, let U_L lie between B_1^2 and H_1^2, and U_R lie in the region indicated in Fig. 4.4. The solution of the Riemann problem for U_L, U_R is the Lax 1-shock wave from U_L to U_M, followed by the fast rarefaction wave from U_M to U_R.

Finally, one can verify that the solution as a function of U_R is continuous in the L_1^{loc} sense in physical space (x, t).

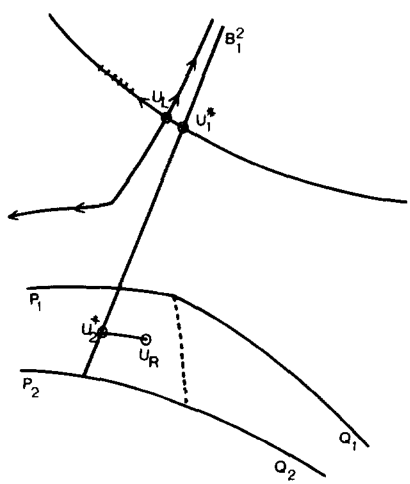

FIGURE 4.3

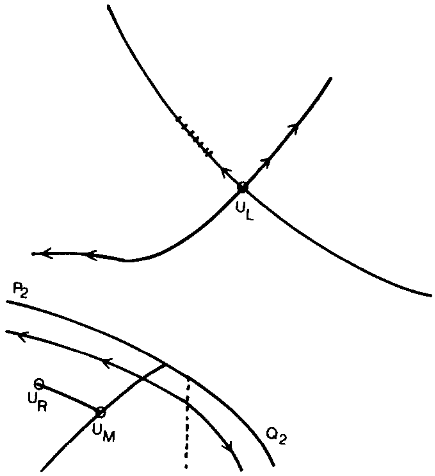

FIGURE 4.4

4.2. *Viscous Profile Shocks*

We prove that there are Lax shocks which do not have viscous profiles. Using theoretical results and numerical experiments, we prove that all shocks of the solutions exhibited in the last section have viscous profiles.

We recall that we have shown that the vector field X_s:

$$\dot{U} = -s(U - U_L) + Q(U) - Q(U_L),$$

associated to the viscosity equation

$$U_t + Q(U)_x = \varepsilon U_{xx}, \qquad \varepsilon > 0,$$

has only two possible configurations in the phase space, when one of the singularities of the vector field is a repeller (or attractor), or equivalently when the vector field has four hyperbolic singularities. The configurations are:

($\mathscr{C}_1$) All three saddles are connected to the repeller (or attractor).

($\mathscr{C}_2$) Only two saddles are connected to the repeller (or attractor).

First, we introduce the concept of structurally stable vector fields. Let $\chi(M^2)$ denote the set of all vector fields of class C^r, $r \geq 1$, on a 2-dimensional compact manifold M^2. Let $\mathscr{B}$ be the space of all vector fields on M^2

with the C^r-topology. A vector field X is structurally stable when a small perturbation in X does not change the topological behavior of its orbits. More specifically:

DEFINITION 4.1. A vector field $X \in \chi(M^2)$ is said to be structurally stable if there is a neighborhood Ω of X in B such that whenever $Y \in \Omega$ there is a homeomorphism $\Phi: M^2 \to M^2$ transforming orbits of X onto orbits of Y.

Consequently, Φ takes singularities of X into singularities of Y and the ω-lim (or α-lim) set of the orbit of X through p is taken into the ω-lim (or α-lim) set of the orbit of Y through $\Phi(p)$.

The next theorem gives a characterization of the vector fields in χ which are structurally stable [13].

THEOREM 4.2. *A vector field $X \in \chi(M^2)$ is structurally stable if and only if it satisfies the following conditions*:

(a) *there are only a finite number of singularities, all hyperbolic*;

(b) *there are only a finite number of closed orbits, all hyperbolic*;

(c) *the ω- and α*-lim *sets of every orbit can only consist of singularities or closed orbits*;

(d) *there are no saddle–saddle connections.*

Moreover, if M^2 is orientable, the set of structurally stable vector fields is open and dense in $\chi(M^2)$.

In order to use this theorem for the vector field X_s (2.4), which is defined on the plane R^2, it is sufficient to consider it on the Poincaré hemisphere Ω, *i.e.*, the hemisphere with equator E defined by the Poincaré transformation as given in Section 2.2. Hence, structurally stable X_s in $\overline{\Omega}$ are characterized as follows [2]:

(i) There are only a finite number of singularities, all hyperbolic;

(ii) there are only a finite number of closed orbits, all hyperbolic;

(iii) there are no saddle–saddle connections.

Since the vector field X_s (2.4), does not have closed orbits it fails to be structurally stable only when either of the singularities are not hyperbolic, *i.e.*, $s = \lambda_i(U)$, $i = 1$ or $i = 2$, where U is a singularity, or there are saddle–saddle connections. By Theorem 2.6, the saddle–saddle connections occur only on a common bifurcation line. Hence, given X_s (i.e., U_L and s) we must verify if two of the singularities of X_s lie on a common bifurcation line and if they are saddles. According to Proposition 4.3, communicated to us by M. Shearer [17], this may happen for a given U_L precisely at points U_1, U_2 where the Hugoniot locus through U_L intercepts a bifurcation line, and s is the common shock speed between U_L and U_1 or U_L and U_2. Of course, this X_s is structurally unstable provided U_1 and U_2 are saddles.

PROPOSITION 4.3. *Let U_L not lie on the bifurcation lines. If the Hugoniot locus through U_L intersects a bifurcation line in two points then these points have the same shock speed.*

Proof. Let U be a point of intersection of $\mathscr{H}_{U_L} = 0$ with a bifurcation line B. Without loss of generality, we assume B is given by $v = \alpha u$. Using (1.4) and (1.6) we get that

$$(\alpha u_L - v_L)F(1,\alpha)u^2 + [G(U_L) - \alpha F(U_L)]u + v_L F(U_L) - u_L G(U_L) = 0. \quad (4.1)$$

Since $U_L \notin B$, we have that $\alpha u_L - v_L \neq 0$. From (4.1), we see that the shock speed

$$s = s(U_L, U) = \frac{F(1,\alpha)u^2 - F(U_L)}{u - u_L} = \frac{\alpha F(U_L) - G(U_L)}{\alpha u_L - v_L},$$

where $U = (1, \alpha)u \in B$, is the same for both roots of (4.1). □

The role of this proposition in the analysis is to show non-profilability of certain Lax shocks in the region between $\widehat{P_1Q_1}$ and $\widehat{P_2Q_2}$ in Fig. 4.1, and thereby to eliminate an otherwise non-unique solution.

To determine which other shocks have viscous profiles numerical results were used to show which of the above configurations $(\mathscr{C}_1)$ and $(\mathscr{C}_2)$, occurred and to localize the states U_L and U_R in this configuration.

For instance, let U_L lie in the region bounded by B_1^2 and H_1^2, and U_{R_1} lie on the Lax 1-shock segment in the disconnected component of the Hugoniot locus and on the left-hand side of B_1^2 (Fig. 4.5). So, U_L is a repeller and U_{R_1} is a saddle. Let U_1 and U_2 be the other saddles on the Lax 1-shock segment in the connected component (Fig. 4.5). In this situation the phase space configuration of the associated vector field is $(\mathscr{C}_1)$, where all saddles are connected to the repeller. Then, all shocks have viscous profiles. Moreover, the vector field is structurally stable, as shown in Fig. 4.6a.

As observed earlier the vector field X_s fails to be structurally stable if either the singularities are not hyperbolic or there is saddle–saddle connection. Moving U_R along the disconnected component of $\mathscr{H}_{U_L} = 0$, in the

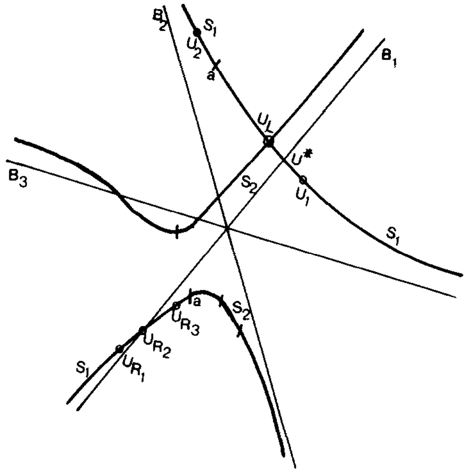

FIGURE 4.5

direction of B_1^2, the associated vector field is not structurally stable when U_R reaches B_1^2. Let U_{R_2} be this intersection. In fact, by Proposition 4.3 another point U^* on the Hogoniot locus is a singularity of the associated vector field X_s, where $s = s(U_L, U_{R_2}) = s(U_L, U^*)$. Using Theorems 2.6–2.8, the saddles U_{R_2} and U^* are connected by an orbit, and U_L and U_{R_2} are not connected by an orbit. Hence, (U_L, U_{R_2}, s) is a Lax 1-shock which does not have a viscous profile (Fig. 4.6b). The other shocks in this figure have viscous profiles.

Now, for U_R on the same disconnected component but on the right side of B_1^2 (e.g., $U_R = U_{R_3}$ in Fig. 4.5) the phase space configuration of X_s is not $(\mathscr{C}_1)$ but $(\mathscr{C}_2)$. In $(\mathscr{C}_2)$, the saddle U_{R_3} is not connected by an orbit to the repeller U_L (Fig. 4.6c). Thus, (U_L, U_{R_3}, s) is a Lax 1-shock which does not have a viscous profile. In this case the vector field X_s is also structurally stable. Moreover, it fails to be stable when continuing to move U_R along the disconnected component of $\mathscr{H}_{U_L} = 0$, U_R fails to be hyperbolic. Hence, the Lax 1-shocks lying on the disconnected component of $\mathscr{H}_{U_L} = 0$, between U_{R_2} and U such that $s(U_L, U) = \lambda_1(U_L)$ do not have viscous profiles.

Similarly, we can get Lax 2-shocks in the connected component of $\mathscr{H}_{U_L} = 0$ (Fig. 4.5), which have viscous profiles. The phase space configurations of X_s is $(\mathscr{C}_1)$. Finally, let U_R lie on the Lax 2-shock segment in the disconnected component of the Hugoniot locus (Fig. 4.5). We can show that U_L and U_R are not connected by an orbit. The phase space configuration of the associated vector field is $(\mathscr{C}_2)$, as was checked numerically, where U_L is the saddle disconnected from the attractor U_R. In this situation the Lax 2-shock segment does not have a viscous profile.

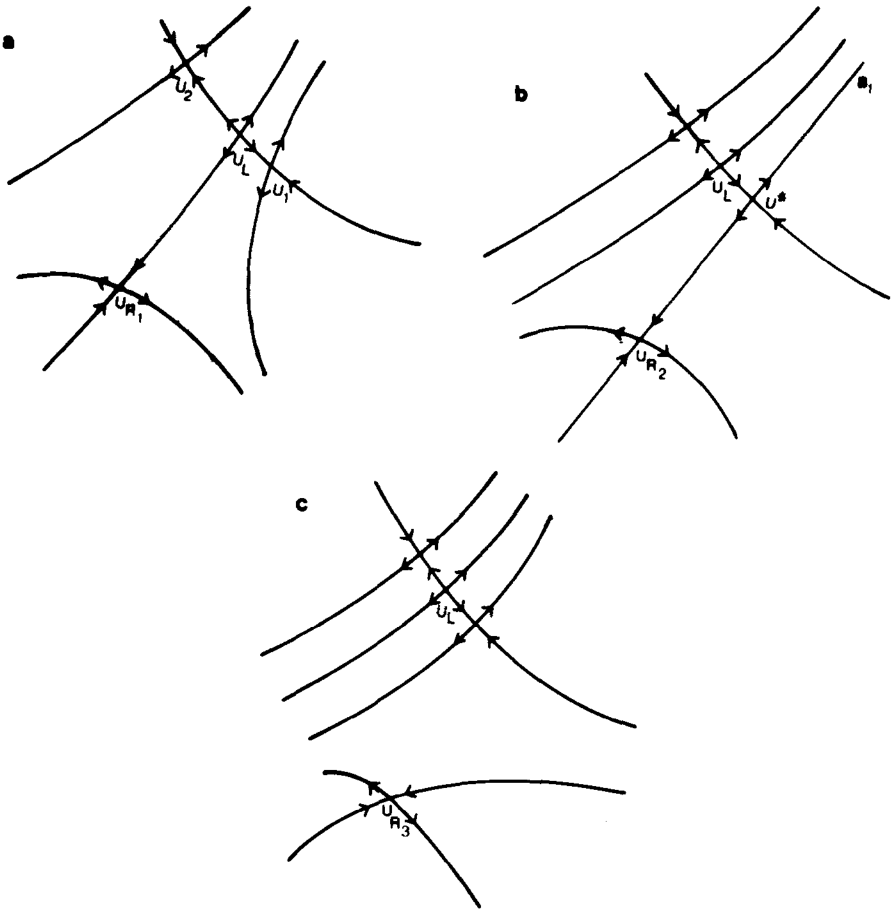

FIGURE 4.6

As shown earlier all profilable crossing shocks are contained on a bifurcation line. These were the only crossing shocks used in the construction of the solutions.

Since we consider $s = \lambda_1(U_L)$ on the construction of a 1-rarefaction-shock composite curve, the vector field X_s has a saddle-node. Thus, it has two more saddles (Theorem 2.3). The saddle-node is a collapse of a saddle with the repeller (or attractor). If this collapse comes from the configuration $(\mathscr{C}_1)$, the saddle-node is connected with both saddles. In another configuration $(\mathscr{C}_2)$, the saddle which is not connected by the repeller (or attractor) continues to be disconnected to the saddle-node. We consider only 1-rarefaction-shock composite curves which have the saddle-node connected to the saddle. Thus, the composite curves which were used on the solution of the Riemann problem, also have viscous profiles.

Now, for $U_L \in B_1^2$ and a choice of parameters (a, b), we prove that the Lax 2-shocks which do not lie on this bifurcation line, do not have viscous profiles.

PROPOSITION 4.4. *Let $C = -\frac{1}{3}u^3 + 2u^2v + uv^2$ be the flux function. Consider $U_L = (1, 1)$ on the bifurcation line $v = u$. The Lax 2-shocks which do not lie on this bifurcation line, do not have viscous profiles.*

Proof. By (1.6), the slopes of the bifurcation lines satisfy

$$\alpha^3 + 4\alpha^2 - 3\alpha - 2 = 0.$$

So, $\alpha = 1$ is the slope of a bifurcation line. The Hugoniot locus through U_L satisfies (1.5),

$$(-u^2 + 4uv + v^2 - 4)(v - 1) - (2u^2 + 2uv - 4)(u - 1) = 0.$$

Then, we have

$$(v - u)(v^2 + 5uv + 2u^2 - v - 3u - 4) = 0.$$

Therefore, the Hugoniot locus through $U_L = (1, 1)$ is the union of the bifurcation line $v = u$ and the hyperbola $v^2 + 5uv + 2u^2 - v - 3u - 4 = 0$. It is easy to see that $U^* = (-\frac{1}{2}, -\frac{1}{2})$ is a secondary bifurcation point, as shown in Fig. 4.7a.

The segments $\{(u, u); -\frac{1}{2} < u < 1\}$ and $\{(u, u); -2 < u < -\frac{1}{2}\}$ are formed by Lax 2-shocks and crossing shocks, respectively. In fact, if U is on the bifurcation line $u = v$, then $\lambda_1(U_L) < s < \lambda_2(U_L)$ and either $\lambda_2(U) < s$ if $-\frac{1}{2} < u < 1$ or $\lambda_1(U) < s < \lambda_2(U)$ if $-2 < u < -1$. Now, we

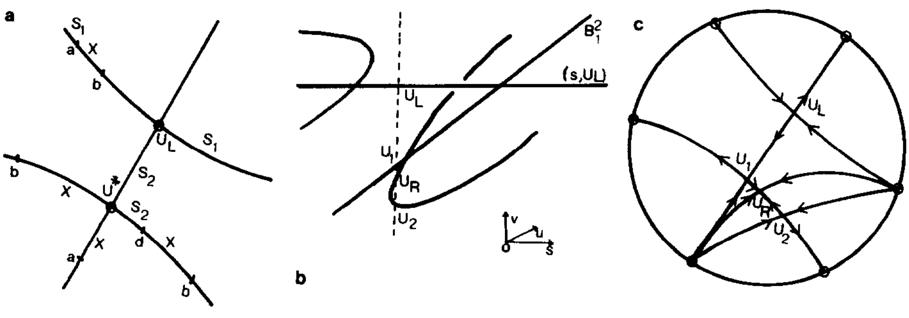

FIGURE 4.7

prove that there is a Lax 2-shock segment on the hyperbola which does not have viscous profile. To show this, it suffices to prove that the derivative of $\lambda_2(U) - s(U_L, U)$ along of the hyperbola, at the point U^* is negative. The hyperbola can be written in polar coordinates as

$$r = -\frac{6(\cos\theta + \sin\theta)}{\sin^2\theta + 5\sin\theta\cos\theta + 2\cos^2\theta}, \theta \neq \arctan\left(\frac{-5 \pm \sqrt{17}}{2}\right),$$

where $u = 1 + r\cos\theta$ and $v = 1 + r\sin\theta$. After some calculations one obtains

$$s = 2 + 6\tan\theta + r\tan\theta\sin\theta + r(4\sin\theta - \cos\theta)$$

and

$$\lambda_2(U)$$
$$= 2\left[1 + r\sin\theta + \sqrt{r^2(2\sin^2\theta + 2\sin\theta\cos\theta + 5\cos^2\theta) + 6r(2\cos\theta + \sin\theta) + 9}\right].$$

Letting the superimposed dot indicate differentiation with respect to θ, we get

$$\dot{r}(\pi) = -\frac{9}{2}, \qquad \dot{s}(U_L, U^*) = -\frac{21}{2}, \qquad \text{and}$$
$$\dot{\lambda}_2(U^*) = -\left(6 + \frac{27\sqrt{2}}{2}\right),$$

where U^* corresponds to $\theta = \pi$ in polar coordinates. Hence, we concluded that $\dot{\lambda}_2(U^*) < \dot{s}(U_L, U^*)$. Consequently, there is a Lax 2-shock segment on this hyperbola.

Finally, we prove that this segment does not have viscous profile. Let U_R be on this Lax 2-shock segment, as shown in Fig. 4.7b. (In this figure the curve lies in $R \times R^2$. The horizontal axis represents s and the vertical axis represents the $U = (u, v)$). Since U_R is an attractor (U_L is a saddle), by Theorem 2.3 the vector field X_s has two other saddles U_1 and U_2 (Fig. 4.7b). Let U_1 be the one on the bifurcation line. Since, both saddles U_L and U_1 are on the bifurcation line, they are connected by an orbit (Theorem 2.6). But, for the vector field X_s having four singularities and saddle–saddle connections there is only one possible configuration (Theorem 2.8), as shown in Fig. 4.7c. In this configuration the attractor U_R is not connected to the saddle U_L. (In this figure there is an one-to-one correspondence between points in the interior of the circle and the (u, v)-plane. The circle itself corresponds to the points at infinity.) □

APPENDIX A

In this Appendix we prove Lemma 2.4 and Theorems 2.7–2.8.

LEMMA A.1. *Let $Q = (F, G)$, where $F(U)$ and $G(U)$ are homogeneous polynomials of degree $2n$, with no common factor, such that* $\det(dQ(U)) < 0$ *for $U \neq 0$. Let X_s be the vector field associated with Q. Then*:

(a) *There exist U_L and s such that the vector field X_s has saddles which are connected by an orbit.*

(b) *All saddles of the vector field X_s lying on a common bifurcation line are connected by an orbit.*

(c) *All saddle–saddle connections of X_s which are straight lines lie on a common bifurcation line.*

Proof. We show that there are two states U_L and U_R on a bifurcation line which are saddles and are connected by an orbit. Let $U_L \neq 0$ lie on a bifurcation line B_i with slope α_i. Since $\det(dQ(U)) < 0 \,\forall\, U \neq 0$ we have that $\lambda_1(U) < 0 < \lambda_2(U)$. Let $U^* = -U_L$. Taking $s(U_L, U^*) = 0$ we see that $U^* \in \mathscr{H}_{U_L}$ since Q is a homogeneous polynomial of even degree. Moreover,

$$\lambda_1(U_L) < s = 0 < \lambda_2(U_L) \qquad \text{and} \qquad \lambda(U^*) < s = 0 < \lambda_2(U^*).$$

Hence s, U_L, U^* is a crossing shock, and therefore exists a segment I containing U^* on B_i such that for all $U \in I$ the shock s, U_L, U is a crossing shock.

Let U_L be one of the saddles lying on the bifurcation line B_i. We claim that if $U_L \neq 0$, this line is an invariant line of the vector field $X_s = (\Phi, \Psi)$ and this vector field restricted to B_i has as its only singularities U_L and U_R. In fact for $U \in B_i$, using (2.4) and (1.4) we have

$$\begin{aligned}
\langle X_s|_{B_i}, (-\alpha_i, 1)\rangle &= -\alpha_i \dot{u} + \dot{v} \\
&= -\frac{v - v_L}{u - u_L}\dot{u} + (v - v_L)\left[-s + \frac{G(U) - G(U_L)}{v - v_L}\right] \\
&= -\frac{v - v_L}{u - u_L}\dot{u} + (v - v_L)\left[-s + \frac{F(U) - F(U_L)}{u - u_L}\right] = 0.
\end{aligned}$$

To verify that $X_s|_{B_i}$ has at most two singularities, we observe that

$$\Phi|_{B_i} = -s(u - u_L) + u^{2n}F(1, \alpha) - F(U_L)$$

has at most two roots. Therefore, if U_L and U_R are on the bifurcation line B_i then B_i is an invariant line and the vector field restricted to B_i has as its only singularities U_L and U_R. Hence, these singularities are connected by an orbit. So we have proven the first two items.

To prove the last item, we must show that if the vector field X_s has an invariant line through a singularity then this line is a bifurcation line. To see this, without loss of generality, let U_L be a saddle. Let $v = \alpha(u - u_L) + v_L$ be an invariant line $\mathscr{L}$. Therefore $\langle X_s|_{\mathscr{L}}, (-\alpha, 1)\rangle \equiv 0$. Consequently we obtain for all $U = u, \alpha(u - u_L) + v_L) \in \mathscr{L}$ we obtain that

$$G(U) - G(U_L) - \alpha[F(U) - F(U_L)] = 0, \qquad \text{(A.1)}$$

or, equivalently,

$$[G(1,\alpha) - \alpha F(1,\alpha)]u^{2n} + P_{2n-1}(u) \equiv 0,$$

where P_{2n-1} is a polynomial of degree $2n - 1$. It follows that the coefficient of u^{2n} is zero, *i.e.*,

$$G(1,\alpha) - \alpha F(1,\alpha) = 0.$$

By (1.6), α is the slope of a bifurcation line. The relation (A.1) implies that this line $\mathscr{L}$ lies on the Hugoniot loci through U_L (1.4). We claim that $\mathscr{L}$ is also a rarefaction curve. In fact, differentiating $\mathscr{H}_{U_L} = 0$ along $\mathscr{L}$ gives $(dQ - (s + \dot{s}M)I)\dot{U} = 0$, where M is a constant. Hence $\dot{U}$ is an eigenvector. Since the system (1.2) is homogeneous the rarefaction curve which is a straight line passes through the origin. Thus $v_L - \alpha u_L = 0$ and the proof is complete. □

Now we determine properties of the vector field X_s restricted to straight lines [2]. We observe that the components Φ and Ψ of the vector field X_s associated with (1.2) are relatively prime polynomials of degree 2.

LEMMA A.2. *Let $X = (\Phi, \Psi)$ be a quadratic vector field on the plane, where Φ and Ψ are relatively prime polynomials.*

(a) *Three singularities of the vector field X are never collinear.*

(b) *If $\mathscr{L}$ is a straight line which is not invariant for the vector field $X = (\Phi, \Psi)$, then X has at most two singularities and point of contacts $\mathscr{L}$. If there are two such points p and q then the orientation of the vector field X in the segment (p, q) is opposite to the orientation of the vector field on the line outside the segment (p, q).*

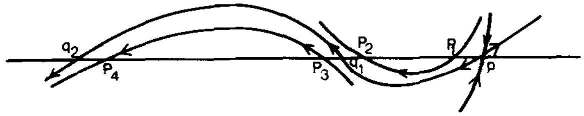

FIGURE A.1

Proof. If the straight line $\mathscr{L}$: $\alpha u + \beta v + \gamma = 0$ contains three singularities then $\mathscr{L}$ intersects each conic $\Phi = 0$ and $\Psi = 0$ in three points. This contradicts the fact that Φ and Ψ are relatively prime.

We suppose that $\mathscr{L}$ is not invariant. The singularity and contact points of X along $\mathscr{L}$ are the solutions of

$$\alpha u + \beta v + \gamma = 0,$$
$$\alpha\Phi(u, v) + \beta\Psi(u, v) = 0.$$

Therefore there are at most two solutions since Φ and Ψ are conics. If there are two distinct points of intersection, p and q, the finite segment (p, q) lies in the region $\alpha\Phi + \beta\Psi < 0$ and both infinite segments lie in the region $\alpha\Phi + \beta\Psi > 0$ or vice versa. □

As a consequence of Lemma A.2 we also prove the lemma below.

LEMMA A.3. *If $\mathscr{L}$ is a straight line through a saddle p of the vector field X_s, the invariant manifolds of p cross $\mathscr{L}$ at most at a single point other than p.*

Proof. Let us assume the contrary, *i.e.*, that there is an invariant manifold of p that crosses $\mathscr{L}$ on the points q_1 and q_2, where q_1 is the first crossing point as we move along this manifold (see Fig. A.1). First assume that q_1 is between p and q_2. By continuity of X_s, there are orbits which cross $\mathscr{L}$ on P_i, $i = 1, 4$, in the direction indicated in Fig. A.1. Thus there are at least two tangents points or singularities of X_s on $\mathscr{L}$, on the segments (P_1, P_2) and (P_3, P_4). This is a contradiction with Lemma A.2. If q_2 is between q_1 and p then we also obtain a contradiction because the vector field along the eigenspace line through a singularity does not change sign at it. More specifically, since the eigenvalues of the linearized system at the critical points are real then either there is an invariant line through this points or the eigenspace straight lines through this point contain no other contacts or singularities and the orientation of the vector field along this line does not change sign at the singularity [2]. □

The theorems below are proven for any vector field X which satisfy the conclusions of Lemma A.2 and Theorem 2.5 and:

(a) X has three saddles and one attractor or repeller, on the finite part of the plane;

(b) X has three attractors and three repellers at infinity;

(c) X neither possesses closed orbits nor singular closed orbits.

In the first theorem we prove that if X_s has four singularities without saddle–saddle connections then there exist two possibilities:

(i) the three saddles are connected to the other singularity which is not a saddle (repeller or attractor) or

(ii) only two saddles are connected to the other singularity which is not a saddle (repeller or attractor).

THEOREM A.4. *Assume that the vector field X_s has four singularities and that there are no saddle–saddle connections. Then at least two saddles are connected to the repeller (or attractor).*

Proof. Without loss of generality, we assume that X_s has three saddles and one repeller.

Let us assume the contrary that there exist two saddles p and q disconnected from the repeller. The idea of the proof is to show that it is not possible to draw the phase space configuration.

Since there are no saddle–saddle connections and there are neither closed orbits nor singular closed orbits, the α-lim and ω-lim sets of the stable and unstable separatrices of p and q are empty sets, as shown in Fig. A.2.

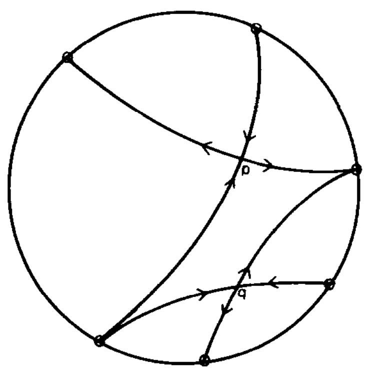

FIGURE A.2

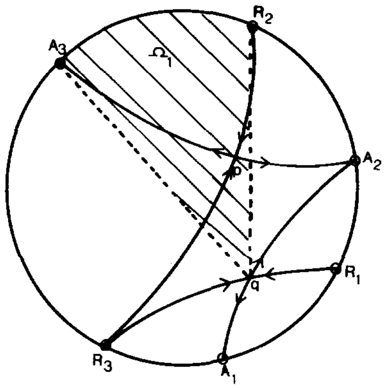

FIGURE A.3

We show that the other saddle σ cannot lie in any of the regions determined by the stable and unstable manifolds of p and q. Let L_1 and L_2 be the straight lines through q in the direction of A_3 and R_2, and Ω_1 the sector determined by L_1 and L_2, as shown in Fig. A.3. Let σ be in Ω_1. Since the straight line through q and σ intersects the stable and unstable manifold of p, there is an orbit tangent to this line. Hence the line contains the singularities q and σ and one tangency point c, in contradiction with Lemma A.2 (Fig. A.4).

Similarly, we conclude that the other saddle cannot lie in the region Ω_2 determined by the straight lines L_3 and L_4 joining p to A_1 and R_1. Therefore, we are left with regions Ω_i, $i = 3, \ldots, 8$, as shown in Fig. A.5.

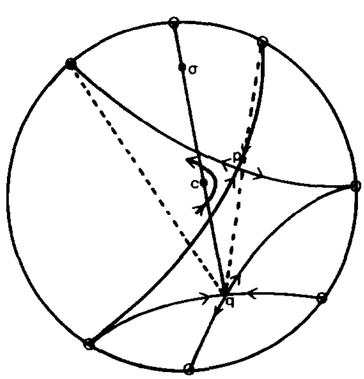

FIGURE A.4

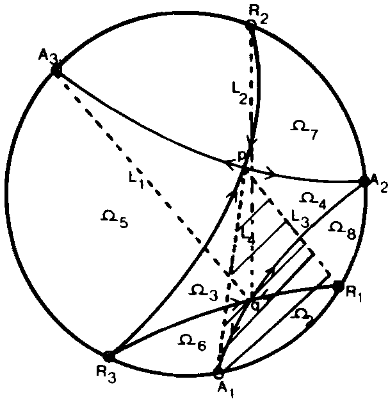

FIGURE A.5

If $\sigma \in \Omega_3$ then the restriction of the vector field to the straight line through q and σ has opposite directions on this line outside the segment (σ, q), as shown in Fig. A.6. By Lemma A.2 this is impossible. Similarly $\sigma \notin \Omega_4$. If $\sigma \in \Omega_5$, joining σ to the other saddles p and q using Lemma A.2 we can find the directions of the separatrices of σ, as shown in Fig. A.7.

Since there are neither attractors nor closed orbits nor singular closed orbits, the unstable separatrices of σ converge to the same attractor at infinity, as shown in Fig. A.8 defining Ω_a.

It is easy to see that the α-lim set of the stable separatrix of σ which is contained in Ω_a is a repeller. Since there are four singularities and there are neither closed orbits nor singular closed orbits, the stable separatrix of σ

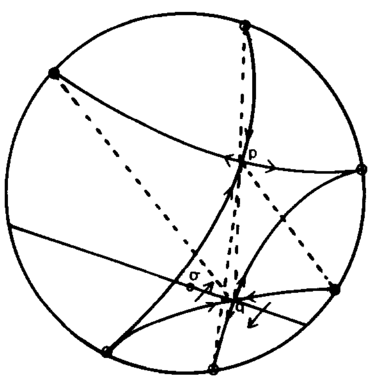

FIGURE A.6

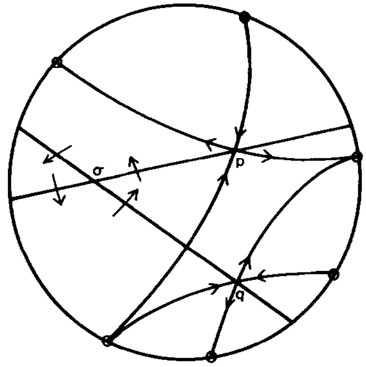

FIGURE A.7

which is not contained in Ω_a tends (at minus infinity) to a repeller at infinity, and hence it crosses the straight line through q and σ in a direction opposite to the vector field orientation, which is a contradiction. We conclude that at least two saddles are connected to the repeller. □

In the next theorem we show that when the vector field has four singularities and there are saddle–saddle connections, there is only one phase space configuration.

THEOREM A.5. *Assume that X_s has four singularities and that there are saddle–saddle connections. Then only two saddles are connected to the repeller (or attractor).*

Proof. Without loss of generality, we assume that a repeller is the singularity which is not a saddle. If there are saddle–saddle connections, by

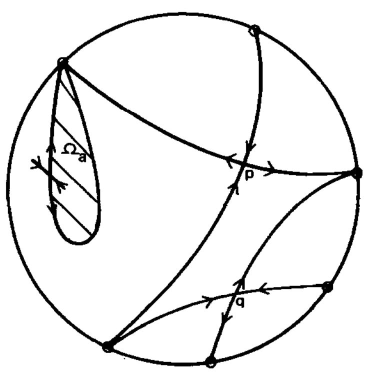

FIGURE A.8

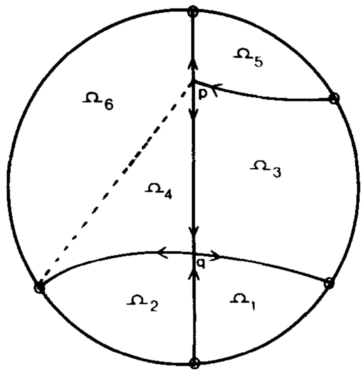

FIGURE A.9

Theorem 2.5 these saddles p and q lie on a bifurcation line B_i. Since the other saddle σ cannot be on B_i, it is neither connected to p nor to q. But there are neither attractors nor closed orbits nor singular closed orbits. Thus the α-lim set of the unstable separatrices of q and at least one of the stable separatrices of p are empty sets.

Let Ω_i, $i = 1, \ldots, 6$ be the regions indicated in Fig. A.9. As in the proof of Theorem A.4, $\sigma \notin \Omega_i$, $i = 1, \ldots, 5$ and the α-lim set of the other stable separatrix γ of p is the repeller r, as shown in Fig. A.10. So suppose $\sigma \in \Omega_6$. Since there are neiter attractors nor closed orbits nor singular closed orbits, separatrices of σ are empty sets. If these separatrices tend to the same attractor at infinity, there is another repeller (Fig. A.11).

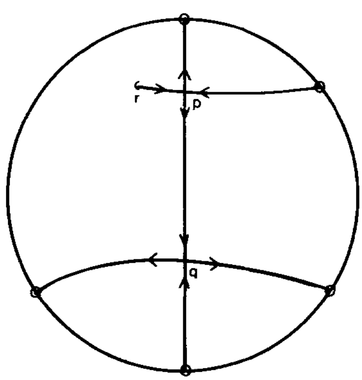

FIGURE A.10

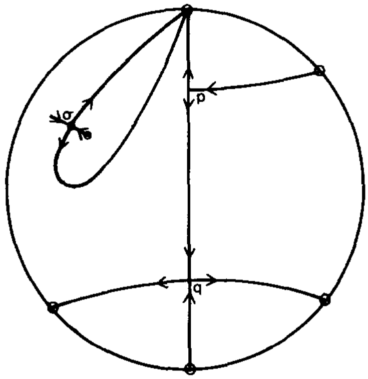

FIGURE A.11

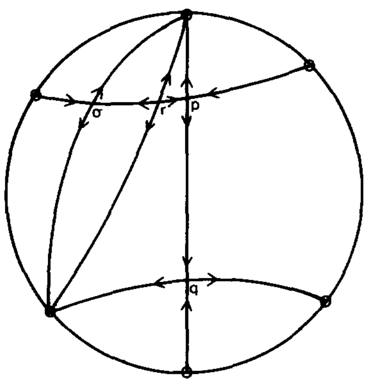

FIGURE A.12

This is impossible. Hence the unstable separatrices of σ tend to different attractors at infinity (Fig. A.12). It is easy to see that σ and r must be connected. □

ACKNOWLEDGMENTS

For the most part, this paper was based on my doctoral thesis. I would like to thank my advisor Dan Marchesin as well as Iaci Malta for many helpful discussions. I would also like to thank Bradley Plohr, Carlos Tomei, and Frederico Furtado for useful suggestions. I wish to thank Professor James Glimm whose constructive criticism helped to improve the development of the article. This work was done while I was at the Courant Institute of Mathematical Sciences.

REFERENCES

1. A. A. ANDRONOV, E. A. LEONTOVICH, I. I. GORDON, AND A. G. MAIER, "Qualitative Theory of Second-Order Dynamics Systems," Wiley, New York, 1966.
2. C. CHICONE, Quadratic gradients on the plane are generically Morse–Smale, *J. Differential Equations* **33** (1979), 159–166.
3. C. CONLEY AND J. SMOLLER, Viscosity matrices for two-dimensional nonlinear hyperbolic systems, *Comm. Pure Appl. Math.* **23** (1970), 867–884.
4. M. G. CRANDALL AND P. H. RABINOWITZ, Bifurcation from simple eigenvalues, *J. Funct. Anal.* **8** (1971), 321–340.
5. I. GEL'FAND, Some problems in the theory of quasi-linear equations, *Uspekhi Mat. Nauk.* **14** (1959), 87–158 (English transl. *Amer. Math. Soc. Transl. Ser. 2* **29** (1963), 295–381.
6. M. E. S. GOMES, "Singular Riemann Problem for a Fourth-Order Model for Multi-Phase Flow," thesis, Departamento de Matematica, Pontificia Universidade Catolica do Rio de Janeiro, 1987. [Portuguese]
7. M. E. S. GOMES, "On Saddle Connections of Quadratic Dynamical Systems with Application to Conservation Laws," in preparation, 1989.
8. E. ISAACSON, D. MARCHESIN, B. PLOHR, AND J. B. TEMPLE, "The Classification of Solutions of Quadratic Riemann Problems (I)," PUC/RJ Report Mat 12/85 and MRC Technical Summary Report 2891, 1985.
9. E. ISAACSON, D. MARCHESIN, B. PLOHR, AND J. B. TEMPLE, Multiphase flow models with singular Riemann problems, in preparation, 1988.
10. P. LAX, Hyperbolic systems of conservation laws II, *Comm. Pure Appl. Math.* **10** (1957), 537–556.
11 J. B. MCLEOD AND D. H. SATTINGER, Loss of stability and bifurcation at a double eigenvalue, *J. Funct. Anal.* **14** (1973), 62–84.
12. J. W. MILNOR, "Topology from the Differentiable Viewpoint," The University Press of Virginia, Charlottesville, VA, 1965.
13. M. M. PEIXOTO, Structural stability on two-dimensional manifolds, *Topology* **1** (1962), 101–120.
14. D. SCHAEFFER AND M. SHEARER, The classification of 2×2 systems of non-strictly hyperbolic conservation laws, with application to oil recovery, *Comm. Pure Appl. Math.* **40** (1987) 141–178.
15. D. SCHAEFFER AND M. SHEARER, Riemann problems for nonstrictly hyperbolic 2×2 systems of conservation laws, *Trans. Amer. Math. Soc.*, 1987.
16. M. SHEARER, D. SCHAEFFER, D. MARCHESIN, AND P. PAES-LEME, Solution of the Riemann problem for a prototype 2×2 system of non-strictly hyperbolic conservation laws, *Arch. Rational Mech. Anal.* **97** (1987), 299–320.
17. M. SHEARER AND S. SCHECTER, Riemann problems involving undercompressive shocks, in "Proceedings, Univ. of Nice, 1988."
18. J. SMOLLER, "Shock Waves and Reaction-Diffusion Equations," Springer-Verlag, New York, 1982.
19. J. A. SMOLLER AND J. L. JOHNSON, Global solutions for an extended class of hyperbolic systems of conservation laws, *Arch. Rational Mech. Anal.*, 1968.
20. B. WENDROFF, The Riemann problem for materials with non convex equations of state. II. General flow, *J. Math. Anal. Appl.* **38** (1972), 640–658.